Development ePress online publication date 20 October 2004

Hes genes regulate size, shape and histogenesis of the nervous system by control of the timing of neural stem cell differentiation

Jun Hatakeyama[1], Yasumasa Bessho[1,*], Kazuo Katoh[2], Shigeo Ookawara[2], Makio Fujioka[3], François Guillemot[4] and Ryoichiro Kageyama[1,†]

[1]Institute for Virus Research, Kyoto University, Kyoto 606-8507, Japan
[2]Department of Anatomy, Jichi Medical School, Tochigi 329-0498, Japan
[3]Kyoto University Graduate School of Medicine, Kyoto 606-8501, Japan
[4]National Institute for Medical Research, Mill Hill, London, NW7 1AA, UK
*Present address: Nara Institute of Science and Technology, Ikoma 630-0101, Japan
†Author for correspondence (e-mail: rkageyam@virus.kyoto-u.ac.jp)

Accepted 9 September 2004

Development 131, 5539-5550
Published by The Company of Biologists 2004
doi:10.1242/dev.01436

Summary

Radial glial cells derive from neuroepithelial cells, and both cell types are identified as neural stem cells. Neural stem cells are known to change their competency over time during development: they initially undergo self-renewal only and then give rise to neurons first and glial cells later. Maintenance of neural stem cells until late stages is thus believed to be essential for generation of cells in correct numbers and diverse types, but little is known about how the timing of cell differentiation is regulated and how its deregulation influences brain organogenesis. Here, we report that inactivation of *Hes1* and *Hes5*, known Notch effectors, and additional inactivation of *Hes3* extensively accelerate cell differentiation and cause a wide range of defects in brain formation. In *Hes*-deficient embryos, initially formed neuroepithelial cells are not properly maintained, and radial glial cells are prematurely differentiated into neurons and depleted without generation of late-born cells. Furthermore, loss of radial glia disrupts the inner and outer barriers of the neural tube, disorganizing the histogenesis. In addition, the forebrain lacks the optic vesicles and the ganglionic eminences. Thus, *Hes* genes are essential for generation of brain structures of appropriate size, shape and cell arrangement by controlling the timing of cell differentiation. Our data also indicate that embryonic neural stem cells change their characters over time in the following order: *Hes*-independent neuroepithelial cells, transitory *Hes*-dependent neuroepithelial cells and *Hes*-dependent radial glial cells.

Key words: Adherens junction, Basal lamina, bHLH, Neuroepithelium, Radial glia, Tight junction

Introduction

Organogenesis involves the initial proliferation process of stem cells and the subsequent differentiation process coupled to withdrawal from the cell cycle. The timing of cell differentiation is thought to be crucial for the size, shape and histogenesis of many tissues, including the brain. In the developing nervous system, neural stem cells (previously known as matrix cells) are initially present as neuroepithelial cells, which proliferate extensively by a symmetric cell division. Around embryonic day (E) 8.5 in mouse, neuroepithelial cells become radial glia by acquiring astroglial features. As neural stem cells, radial glia give rise to neurons first and glial cells later (Fujita, 1964; McConnell, 1995; Temple, 2001). During neurogenesis, radial glial cells are known to undergo an asymmetric cell division, by which each radial glial cell forms one neuron and one radial glial cell.

The size and shape of the nervous system largely depend on how many times neural stem cells re-enter the cell cycle (Ohnuma and Harris, 2003). For example, the brain becomes enlarged when cell differentiation is delayed by null mutation for the cyclin-dependent kinase (CDK) inhibitor p27Kip1, which inhibits cell cycle progression (Fero et al., 1996; Nakayama et al., 1996), or by misexpression of a stabilized β-catenin, an effector for Wnt signalling, which induces cell proliferation (Chenn and Walsh, 2002). The timing of cell differentiation may also influence cell fate choice, because neural stem cells change their competency over time during development (McConnell, 1995; Qian et al., 2000; Temple, 2001). However, although delayed cell differentiation by misexpression of a stabilized β-catenin increases neurons as well as neural stem cells, the enlarged brain with massive expansion of the cortex has a normal spatial pattern of neuronal differentiation (Chenn and Walsh, 2002). Thus, it is still obscure how the timing of cell differentiation influences cell fate choice and the histogenesis of the nervous system. Conversely, acceleration of cell differentiation was also attempted by disrupting cyclin D and cyclin E genes, which are believed to play an essential role in cell cycle progression (Sherr and Roberts, 1999). However, unexpectedly the defects of these cyclin-null mice are mild and occur only at late stages (Fantl et al., 1995; Huard et al., 1999; Sicinski et al., 1995; Geng et al., 2003). Thus, it remains to be determined whether premature cell differentiation simply generates small tissues

with mostly normal shapes and histology or significantly affects the structures.

The basic helix-loop-helix genes *Hes1* and *Hes5* are essential effectors for Notch signalling, which regulates the maintenance of undifferentiated cells (Artavanis-Tsakonas et al., 1999; Gaiano and Fishell, 2002; Hitoshi et al., 2002; Honjo, 1996; Kageyama and Nakanishi, 1997; Selkoe and Kopan, 2003). Hes1 represses expression of the CDK inhibitor p21Cip1 (Castella et al., 2000; Kabos et al., 2002) and functionally antagonizes differentiation genes such as *Mash1*, thus controlling both cell cycle and differentiation. We previously reported that *Hes1* and *Hes5* play an important role in maintenance of neural stem cells (Tomita et al., 1996; Nakamura et al., 2000; Ohtsuka et al., 2001; Cau et al., 2000). Here, we examined the defects of the nervous system of embryos lacking *Hes1* and *Hes5* in more detail. We also examined embryos additionally lacking *Hes3*, which has a similar activity to that of *Hes1* and *Hes5* (Hirata et al., 2000). In these mutants, virtually all neural stem cells prematurely differentiate into neurons only without generating the later-born cell types, and the brain structures are severely destroyed. These results indicate that control of the timing of cell differentiation by *Hes* genes is essential not only for the size and shape, but also for the structural integrity, of the nervous system.

Materials and methods

Hes1$^{-/-}$, *Hes3*$^{-/-}$ and *Hes5*$^{-/-}$ mutant mice

All animals used in this study were maintained and handled according to protocols approved by Kyoto University. Genotypes of *Hes1*$^{-/-}$, *Hes3*$^{-/-}$, and *Hes5*$^{-/-}$ embryos (Cau et al., 2000; Hirata et al., 2001) were determined, as described previously (Hirata et al., 2001; Ohtsuka et al., 1999).

Scanning electron microscopic analysis

Embryos were fixed in 2.0% glutaraldehyde in 0.1 M phosphate buffer for 24 hours at 4°C and then washed three times in 0.1 M phosphate buffer for 10 minutes each. They were mounted in 4% Sea Plaque GTG agarose (FMC) and the gel was removed after cutting. Samples were dehydrated with alcohol of a series of increasing concentrations to 100%. Embryos were then freeze-dried, mounted onto metal stubs with carbon-conductive paint, coated with a thin layer of gold using a sputter coater (Eiko IB-3), and viewed using a scanning electron microscope (SEM; Hitachi S-450).

Transmission electron microscopy analysis

Embryos were perfusion-fixed with 2.5% glutaraldehyde and 2% paraformaldehyde in 0.1 M sodium cacodylate buffer, pH 7.2. The embryos were cut transversely into small pieces, and the samples including upper limb and spinal cord were further fixed in fresh fixative for 3 hours at room temperature and then overnight at 4°C. After being washed in 0.1 M sodium cacodylate buffer, the specimens were post-fixed with 1% OsO_4 for 2 hours on ice, stained en bloc with 0.5% uranyl acetate for 2 hours, and then dehydrated and embedded in Epon 812. Ultrathin sections (80 nm) were cut and examined using a JEOL JEM 2000 EX-type electron microscope operated at 80 kV.

In-situ hybridization

For in-situ hybridization, antisense strand probes were labelled with digoxigenin, as previously described (Hirata et al., 2001).

Histochemical analysis

Embryos were fixed, as previously described (Hatakeyama et al., 2001). Alternatively, embryos were fixed at 4°C in 10% trichloroacetic acid solution for 1 hour, washed in PBS, and embedded in OCT (Hayashi et al., 1999). Embedded embryos were sectioned by a cryostat at 16 μm.

Immunochemistry was done, as previously described (Hatakeyama et al., 2001), with the following antibodies: anti-N-cadherin (BD Transduction Laboratories), anti-RC2 (Hybridoma Bank), anti-nestin (Pharmingen), anti-TuJ1 (Babco), anti-Ki67 (Pharmingen), anti-laminin-α1 (Chemicon), anti-ZO-1 and anti-claudin-10, -15 and -18, which were kindly provided by Dr Shoichiro Tsukita (Kiuchi-Saishin et al., 2002). TdT-mediated dUTP nick-end labelling (TUNEL) assay was performed with a detection kit (Roche).

Toxin-induced cell ablation

For pNes-DT-A and pNes-GFP, cDNAs for diphtheria toxin A subunit (DT-A) (Yamaizumi et al., 1978) and EGFP, respectively, were inserted between the nestin promoter and intron II, a CNS-specific enhancer. Electroporation was performed, as previously described (Ohtsuka et al., 2001). Square electroporator CUY21 EDIT (TR Tech) was used to deliver five 50-ms pulses of 30 V with 950-ms intervals.

Results

Compensatory expression of *Hes1* and *Hes5*

We first examined the expression patterns of *Hes1* and *Hes5* in mouse embryos. These two genes were widely expressed in the developing nervous system, but their expression patterns were rather complementary to each other (Fig. 1A-E,G,I). For example, *Hes5* was strongly expressed in the midbrain and hindbrain but not in the isthmus, while *Hes1* was expressed in the isthmus (Fig. 1A,B, arrowheads). In the optic vesicle, *Hes1* but not *Hes5* was expressed (Fig. 1C-E, arrows). Interestingly, in the absence of either *Hes1* or *Hes5*, expression of the remaining *Hes* gene was upregulated in many regions. For example, *Hes5* expression was observed in the optic vesicles of *Hes1*-null embryos (Fig. 1F, arrow). Similarly, *Hes1* and *Hes5* expression was expanded in the spinal cord of *Hes5*-null (Fig. 1H, arrows) and *Hes1*-null (Fig. 1J, arrow) embryos, respectively. This compensatory expression may explain weak or no apparent defects in *Hes1*-null or *Hes5*-null embryos, in contrast to those lacking both *Hes1* and *Hes5* (Fig. 2A-D). We thus examined the double-mutant mice in more detail to understand the significance of the timing of cell differentiation. *Hes1;Hes5* double-mutant embryos survived until E10.5, and their defects were more specific to the nervous system than those of *Notch*-mutant mice (Swiatek et al., 1994; Conlon et al., 1995; Hamada et al., 1999).

Disorganization of the neural tube morphology in *Hes1-Hes5* double-mutant mice

Scanning electron microscopic (SEM) analysis revealed that at E10.5, cells were radially aligned throughout the wall of the wild-type neural tube (Fig. 2E,F). The endfeet of these cells were tightly connected each other, forming a smooth inner surface (Fig. 2I). By contrast, in *Hes1;Hes5* double mutants, cell arrangement was severely disorganized, with many cells scattered into the lumen of the neural tube (Fig. 2G,H). These cells had lost radial morphology but had become round in shape (Fig. 2J, compare with Fig. 2I). Furthermore, the outer boundary of the neural tube was also irregular and ambiguous in the double mutant (Fig. 2G). Thus, *Hes1* and *Hes5* are essential for the structural integrity of the embryonal nervous

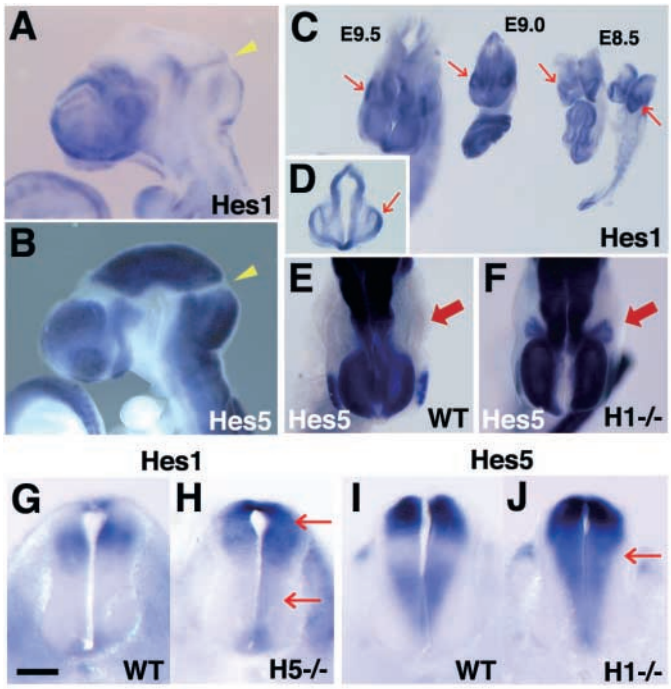

Fig. 1. *Hes1* and *Hes5* expression in the developing nervous system. In-situ hybridization for *Hes1* and *Hes5* was performed with mouse embryos at E9.5 or indicated stages. (A-E) *Hes1* and *Hes5* exhibit mostly complementary expression patterns. *Hes1* is expressed in the isthmus (A, arrowhead) and the optic vesicles (C,D, arrows) whereas *Hes5* is not (B, arrowhead and E, arrow). (F) In the *Hes1*-null embryo, *Hes5* is expressed in the optic vesicles (arrow). (G-J) *Hes1* and *Hes5* exhibit complementary expression patterns in the spinal cord. *Hes1* and *Hes5* expression is expanded in *Hes5*-null (H, arrows) and *Hes1*-null spinal cord (J, arrow), respectively. The dorsal is up in G-J. Scale bar: 50 μm in G-J.

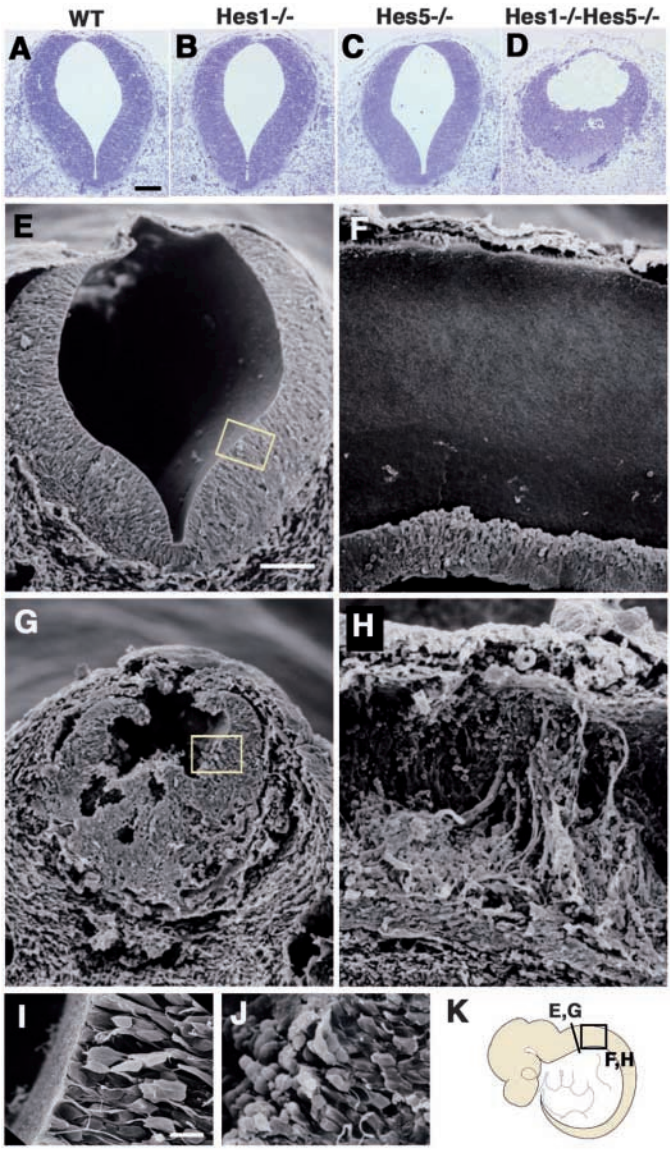

Fig. 2. Disorganized structures of the *Hes*-mutant nervous system. (A-D) Toluidine Blue staining of sections at the level of rhombomere 7 of wild-type (A), $Hes1^{-/-}$ (B), $Hes5^{-/-}$ (C) and $Hes1^{-/-}$;$Hes5^{-/-}$ (D) at E10.5. Only $Hes1^{-/-}$;$Hes5^{-/-}$ neural tube is morphologically abnormal. In these panels, dorsal is up. (E-J) SEM analysis was performed with E10.5 mouse embryos. (E,F,I) In the wild type, radial glial cells are aligned radially in the wall of the neural tube. Their endfeet form a smooth inner surface. (G,H,J) In *Hes1;Hes5* double mutants, cells are exposed to, and scattered into, the lumen. As a result, the cell arrangement is totally destroyed. In addition, cells become round in shape (J, compare with I). Boxed regions in (E,G) are enlarged in (I,J). (K) Positions of (E-H) are indicated. Scale bars: 100 μm in A-H; 10 μm in I,J.

system. We observed this defect along the entire anterior-posterior axis of the spinal cord all the way to the diencephalon but not in the telencephalon at E10.5 (see below), which may reflect slower development in the telencephalon than in other regions. Because almost all the double-mutant embryos died by E11, we were not able to examine the defects of the telencephalon at later stages.

To investigate whether cell death is involved in the disorganized cell arrangement in *Hes1;Hes5* double mutants, we next performed TUNEL assay. During E8.5-E10.5, there was no significant increase of $TUNEL^+$ cells in the double-mutant spinal cord (Fig. 3A-F), indicating that the structural disorganization was not due to cell death. In addition, the floor plate (Shh^+), V3 interneurons ($Sim1^+$), V0 interneurons ($Evx1^+$), D1A interneurons ($Lhx2^+$), and the roof plate ($Wnt1^+$) were generated in the double-mutant spinal cord as in the wild type (Fig. 3G-P), suggesting that the dorsal-ventral patterning is mostly normal in the absence of *Hes1* and *Hes5*, despite the severe morphological abnormalities.

Premature neuronal differentiation and concomitant loss of radial glia in *Hes*-mutant mice

To further characterize the defects of *Hes1;Hes5* double-mutant embryos, we performed immunohistochemistry. At E8.5, the neural plate consisted of $nestin^+$ neuroepithelial cells in *Hes1;Hes5* double-mutant embryos as in the wild type (Fig. 4A,D). At E9.5 and 10.5, when neuroepithelial cells became radial glia and neurogenesis actively occurred, $nestin^+$ radial glial cells were radially aligned throughout the wall of the spinal cord in the wild type (Fig. 4B,C). By contrast, in the double mutant, $nestin^+$ radial glial cells were prematurely lost from the ventral region (Fig. 4E,F). Furthermore, they were also decreased in the dorsal region at E10.5 (Fig. 4F). These

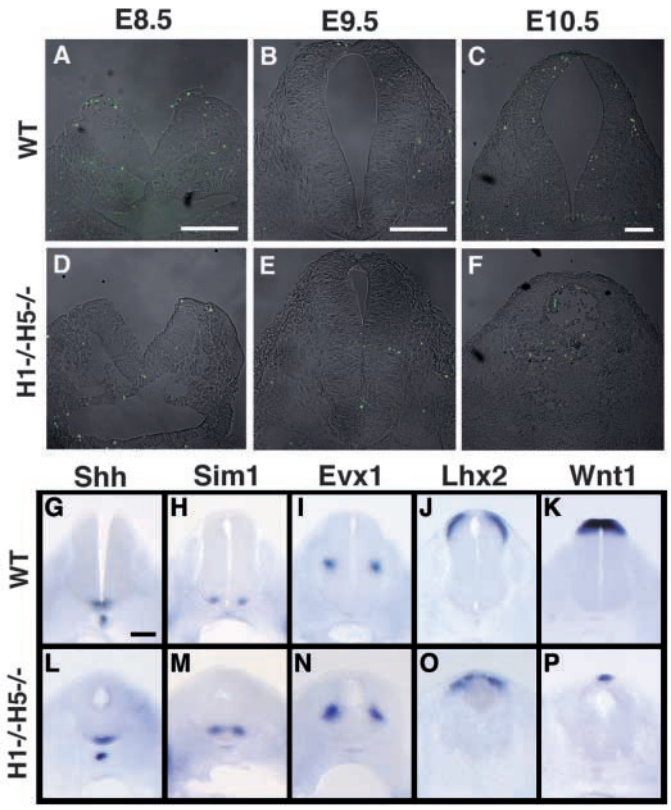

Fig. 3. Cell death and dorso-ventral patterning of the spinal cord. (A-F) TUNEL assay indicates that cell death (green) is not increased in *Hes1*$^{-/-}$*Hes5*$^{-/-}$ spinal cord (D-F). (G-P) In-situ hybridization analysis of *Shh* for the floor plate (G,L), *Sim1* for V3 interneurons (H,M), *Evx1* for V0 interneurons (I,N), *Lhx2* for D1A interneurons (J,O), and *Wnt1* for the roof plate (K,P) at E10.5. Except for the hypomorphic roof plate, the dorso-ventral patterning is mostly normal in *Hes1*$^{-/-}$*Hes5*$^{-/-}$ spinal cord (L-P). Scale bars: 100 μm.

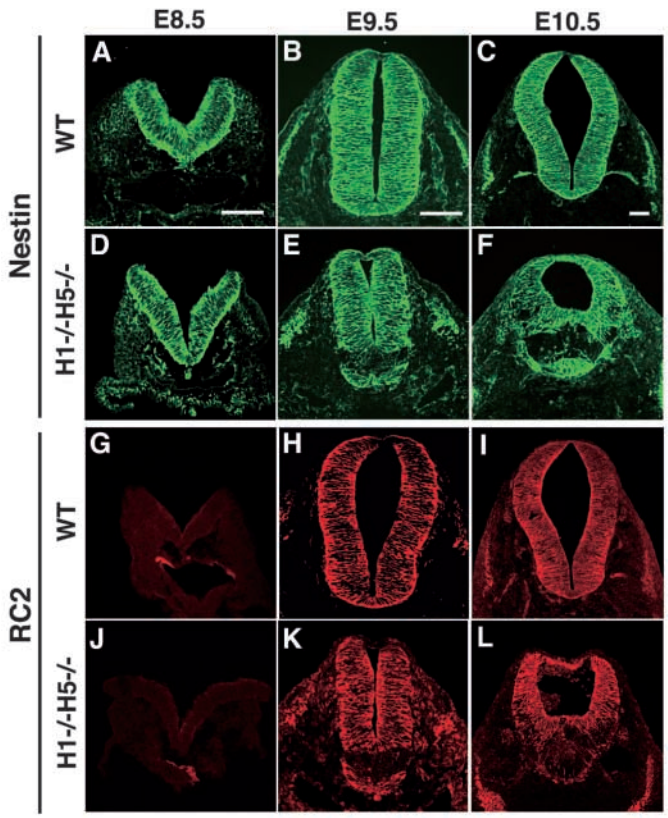

Fig. 4. Premature loss of radial glia in *Hes*-mutant spinal cord. Histological analysis was done with the wild-type (A-C,G-I) and *Hes1;Hes5* double-mutant (D-F,J-L). The dorsal is up in all panels. At E8.5, the neural plate consists of nestin^{+} neuroepithelial cells in *Hes1;Hes5* double-mutant (D) as in the wild type (A). At E9.5 and E10.5, nestin^{+}RC2^{+} radial glial cells are present throughout the wall of the spinal cord in the wild type (B,C,H,I). By contrast, in the double mutant, nestin^{+}RC2^{+} radial glial cells are prematurely lost from the ventral region (E,F,K,L). Scale bars: 100 μm.

results indicate that in the double mutant, although neuroepithelial cells are normally formed, radial glial cells are prematurely lost. Agreeing with this notion, expression of the radial glial marker RC2 was also lost from the ventral region at E9.5 and 10.5 (Fig. 4K,L).

We next examined the differentiation status in the double mutant. In the wild type, radial glial cells, which were mitotically active (Ki67^{+}), were present throughout the wall of the spinal cord, while neurons (TuJ1^{+}) resided in the outer layer at E10.5 (Fig. 5A). By contrast, in the double mutant, Ki67^{+} radial glial cells were depleted from the ventral region and, instead, this region was occupied by prematurely differentiated TuJ1^{+} neurons (Fig. 5E). Expression of the Notch ligand gene *Dll1* and the proneural bHLH genes *Mash1* and *Math3*, all of which are expressed by differentiating neurons, was highly upregulated in the double mutant (Fig. 5F-H), compared to the wild type (Fig. 5B-D) at E9.25. It is likely that this upregulation of the proneural bHLH genes may be responsible for accelerated neurogenesis in the double mutant. In these mutants, the later-born cells, such as oligodendrocytes, astrocytes and ependymal cells, were not generated (data not shown). Because there was no significant increase of TUNEL^{+} cells in the mutants (Fig. 3D-F), the lack of the later-born cell types was not due to cell death. It is likely that, in the absence of *Hes* genes, radial glial cells are prematurely differentiated into neurons at the expense of late-born cells, indicating that *Hes* genes are essential for generation of a full range of cell types.

Loss of the junctional complex in *Hes1-Hes5* double-mutant spinal cord

To determine how the structural defects occur in *Hes1;Hes5* double mutants, we examined the junctional complex. Transmission electron microscopy (TEM) studies showed that the adherens junction and the tight junction were formed at the apical side of neuroepithelial cells in both the wild type and the double mutant at E8.5 (Fig. 6B,E, arrowheads). A higher magnification shows kissing points of the tight junction (Fig. 6C,F, arrows). Consistent with this observation, the tight junction molecules claudin-10, -15 and -18 (Tsukita et al., 2001), as well as the adherens junction molecule N-cadherin (Hatta and Takeichi, 1986), were expressed at the apical surface of neuroepithelial cells of both the wild type and the double mutant (Fig. 6G-L and data not shown). Thus, the structural integrity of the neuroepithlium was maintained at E8.5 in *Hes1;Hes5* double mutants.

At E9.5-10.5, the tight junction and the adherens junction

were observed at the apical side of radial glial cells in the wild-type spinal cord (arrows, brackets and arrows in Fig. 7E,J,K, respectively). In addition, the tight junction molecule claudin and the adherens junction molecule N-cadherin were expressed at the apical surface of radial glial cells (Fig. 7G-I,L-N and data not shown). By contrast, in *Hes1;Hes5* double mutants, cells of the right and left walls of the neural tube were intermingled with each other (Fig. 7B,D) and lacked the junctional complex at E9.5 (arrowheads and arrows in Fig. 7F,O-Q, respectively). This region was occupied by prematurely differentiated neurons (TuJ1$^+$) (Fig. 7P, arrow). Thus, radial glial cells, which form the apical intercellular junctions, were prematurely differentiated into neurons in the double mutant, and this loss of the junctional complex seemed to allow neurons to scatter into the lumen.

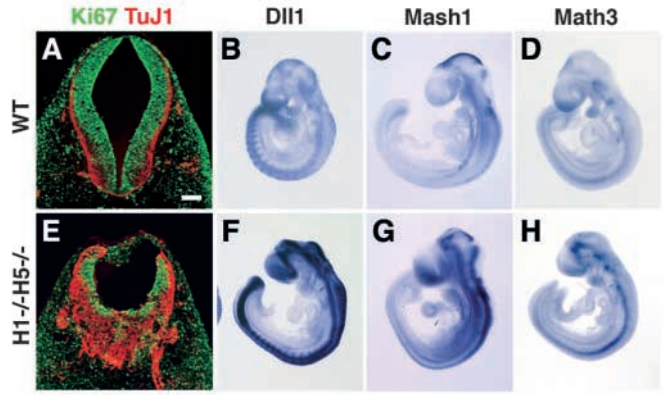

Fig. 5. Premature neurogenesis in *Hes1;Hes5* double mutants. (A) In the wild type, radial glial cells (Ki67$^+$) are located throughout the wall while neurons (TuJ1$^+$) reside in the outer layer at E10.5. (E) In *Hes1;Hes5* double mutants, there are numerous neurons (TuJ1$^+$) while radial glial cells (Ki67$^+$) are significantly decreased. (B-D,F-H) In-situ hybridization analysis shows that expression of *Dll1*, *Mash1* and *Math3* is highly upregulated in *Hes1;Hes5* double mutants (F-H), compared with the wild type (B-D). Scale bar: 100 μm in A,E.

Loss of the basal lamina in *Hes1-Hes5* double-mutant spinal cord

Because neurons (TuJ1$^+$) had escaped from the neural tube into the surrounding region (Fig. 8E,G,H, arrowheads), it is likely that the outer barrier was also affected in the double mutant. The outer boundary of the neural tube was demarcated by the basal lamina in the wild type (Fig. 8B, open arrows). By contrast, the basal lamina was undetectable in the ventral spinal cord of the double mutant (Fig. 8F, arrows). Furthermore, many neurons of the spinal cord and the dorsal root ganglia were intermingled with each other in the double mutant (Fig. 8D,G, arrows). In the wild type, the basal lamina glycoprotein laminin-α1 was expressed at the basal boundary (Fig. 8I-K). However, in the double mutant, laminin-α1 expression was lost or severely disorganized in the ventral region, where radial glial cells (nestin$^+$) were depleted (Fig. 8M-O), while the expression was still intact at the dorsal boundary, where radial glial cells still remained (Fig. 8M-O). Thus, premature loss of radial glial cells led to defects of the basal lamina. In-situ hybridization analysis demonstrated that laminin-α1 mRNA was expressed in the ventricular zone of the wild type, where cell bodies of radial glial cells were present (Fig. 8L), as previously described (Thomas and Dziadek, 1993). By contrast, expression of laminin-α1 mRNA was undetectable in the ventral spinal cord of the double mutant (Fig. 8P). These results indicate that the loss of radial glia leads to disruption of the basal lamina, allowing neurons to escape into the surrounding regions. Taken together, radial glial cells are essential for the structural integrity of the nervous system by forming the apical and basal barriers.

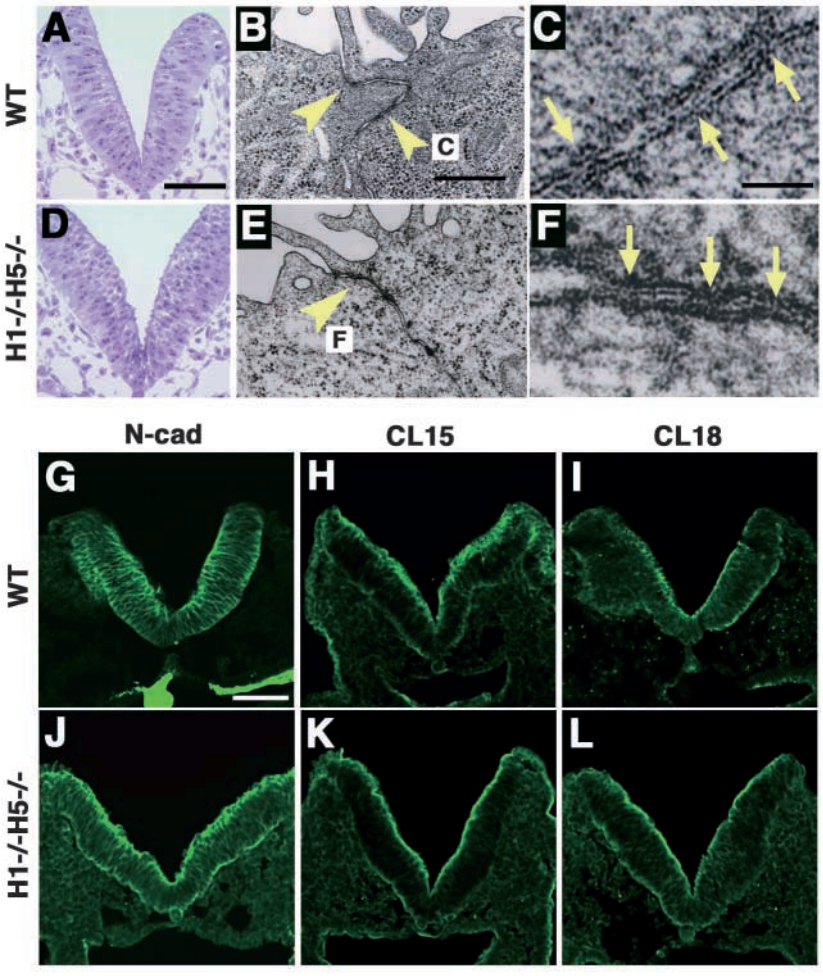

Fig. 6. Formation of the intercellular junctional complex at the apical side of the neuroepithelium. (A,D) Toluidine Blue staining of the wild-type and *Hes1;Hes5* double-mutant neuroepithelium at E8.5. (B,C,E,F) TEM analysis of the wild-type and *Hes1;Hes5* double-mutant neuroepithelium at E8.5. The junctional complex (arrowheads) is formed at the apical side of the neuroepithelium in both wild-type (B,C) and *Hes1;Hes5* double-mutant embryos (E,F). Kissing points of the tight junction are indicated by arrows (C,F). (G-L) At E8.5, the adherens junction molecule N-cadherin and the tight junction molecules claudin-15 and -18 are expressed at the apical side of the neuroepithelium in both wild-type (G-I) and *Hes1;Hes5* double-mutant embryos (J-L). Scale bars: 100 μm in A,D,G-L; 500 nm in B,E; 50 nm in C,F.

Ablation of radial glial cells destroys the structural integrity of the neural tube

The above results show that premature loss of radial glia abolished the inner and outer barriers and allowed neurons to escape into the lumen and the surrounding regions. These results point to the importance of radial glia in the maintenance of neural tube morphology. To further confirm this notion, we next ablated radial glial cells by expressing diphtheria toxin (DT) under the control of the nestin promoter/enhancer (pNes-DT-A) (Fig. 9H). This promoter/enhancer directed specific expression in nestin$^+$ radial glial cells (Fig. 9I-L) (Zimmerman et al., 1994). We injected pNes-DT-A into the ventricle of embryonal telencephalon at E13 and performed electroporation, which introduced the vector into the cells on the plus side. To identify the transfected region, we co-injected the vector for GFP expression under the control of the CMV promoter/enhancer (pCL-GFP) (Fig. 9D), which allowed ubiquitous GFP expression (Fig. 9A). After five days (E18), introduction of pCL-GFP alone stained both radial glia and neurons (Fig. 9O) and did not affect expression of the apical junction molecule ZO-1 (Fig. 9Q, arrowheads), the basal lamina (laminin α1) (Fig. 9N, arrowheads) or neuronal arrangement (NeuN) (Fig. 9R). By contrast, when pNes-DT-A was introduced, we found many TUNEL$^+$ cells only in the ventricular zone after 2 days (E15) (Fig. 9E-G), indicating that the pNes-DT-A vector specifically killed nestin$^+$ radial glial cells. Furthermore, after five days (E18), the electroporated region had lost radial glial cells (nestin$^+$) (Fig. 9V,V′, arrowheads) while it contained a small number of GFP$^+$ neurons (Fig. 9T,T′), which were probably nestin-negative differentiating neurons at the time of electroporation. This region lost expression of ZO-1 at the apical side (Fig. 9W, arrowheads) and laminin α1 at the basal side (Fig. 9X, between the two arrowheads). Instead of radial glial cells, the ventricular zone was occupied by ectopic neurons (NeuN$^+$), which were scattered into the ventricle (Fig. 9Y,Y′, arrowheads). Furthermore, the cortical lamination was destroyed with rosette-like structures, and some neurons protruded into the outer region through the area that lacked laminin α1 expression (Fig. 9U,X,Y). These abnormalities were very similar to those of *Hes1;Hes5* double-mutant spinal cord, supporting the notion of the important roles of radial glia in maintenance of the structural integrity.

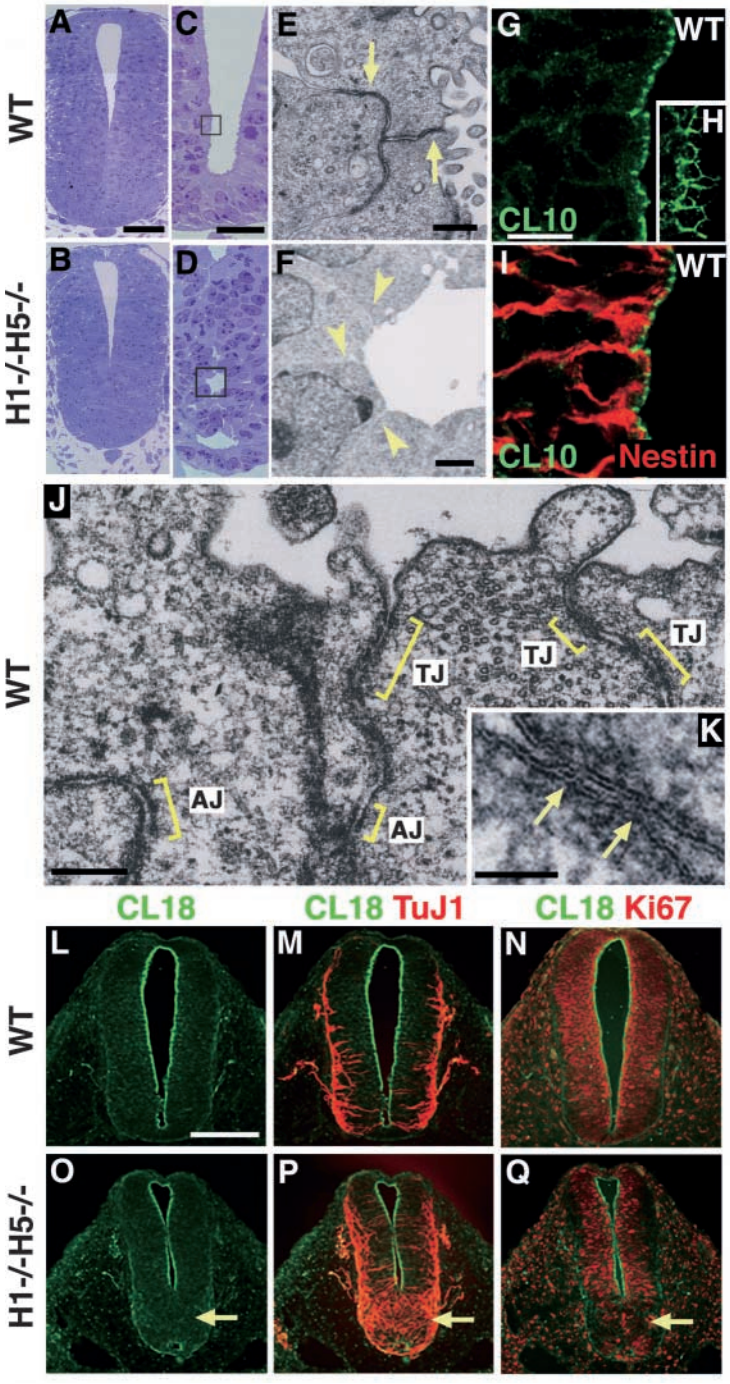

Eyes are not formed in *Hes1;Hes5* double-mutant embryos

Similar but less severe defects were also observed in the mesencephalon and diencephalon of *Hes1;Hes5* double-mutants (Fig. 10B, arrows). Although the forebrain was less severely affected, it became a rather monotonous tube, compared with the wild type (Fig. 10A,B). Strikingly, *Hes1;Hes5* double-null embryos had no optic vesicles (Fig. 10B,I, compare with Fig. 10A, arrow, and H). In the wild-type optic vesicles, neuronal differentiation did not occur at

Fig. 7. Premature loss of the apical intercellular junctions in *Hes1;Hes5* double-mutant spinal cord. (A-D) Sections of the wild type (A,C) and *Hes1;Hes5* double mutant (B,D) at E9.5. Cells in the right and left walls of the double mutant are intermingled (D). (E,F) TEM analysis revealed the junctional complex at the apical side of the wild type (E, arrows). By contrast, the junctional complex is already lost in the *Hes1;Hes5* double mutant (F, arrowheads). The boxed regions in C,D are enlarged. (G-I) Claudin-10 is expressed at the apical side of radial glia (nestin$^+$) in the wild type. The en face view of the ventricular surface shows a ring-like distribution of claudin-10 (H). (J,K) TEM analysis shows the tight junction (kissing points are indicated by arrows in K) and adherens junction at the apical side in the wild type (J, brackets). (L-N) Claudin-18 is expressed at the apical side of radial glia (Ki67$^+$) while neurons are located in the outer region (TuJ1$^+$). (O-Q) In the double mutant, claudin-18 expression is lost in the ventral region, where radial glial cells are depleted (Q, arrow). This region is occupied by TuJ1$^+$ neurons (P, arrow). Scale bars: 50 μm in A,B; 25 μm in C,D; 500 nm in E; 1 μm in F; 10 μm in G-I; 300 nm in J; 70 nm in K; 100 μm in L-Q.

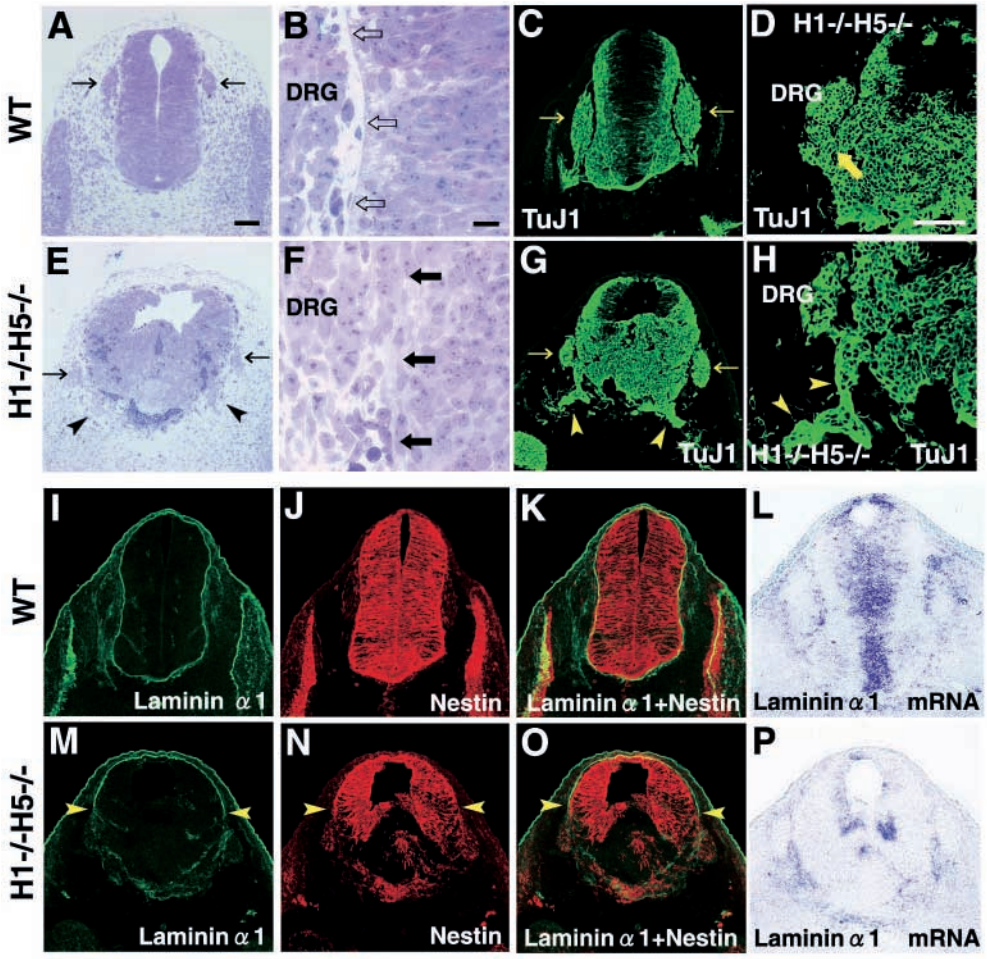

Fig. 8. Premature loss of the basal lamina in the *Hes1;Hes5* double mutant. (A) In the wild type, the spinal cord and dorsal root ganglia (DRG, arrows) are clearly separated. (B) The basal lamina is formed at the outer barrier of the wild-type spinal cord (open arrows). (C) Neurons (TuJ1$^+$) in the spinal cord and DRG (arrows) are clearly separated in the wild type. (D) In the double mutant, neurons (TuJ1$^+$) in the spinal cord and DRG are intermingled (arrow). (E) In the double mutant, the outer boundary of the spinal cord is not clear. Some cells are erupted from the spinal cord (arrowheads). (F) The basal lamina is not formed at the boundary of the double-mutant spinal cord (arrows). (G,H) Neurons (TuJ1$^+$) are erupted from the spinal cord (arrowheads), and some of them are intermingled with the DRG. (I-K) Laminin-α1 is expressed at the basal side of radial glia (nestin$^+$) in the spinal cord. (L) Laminin-α1 mRNA is expressed in the ventricular zone. (M-O) In the double mutant, laminin-α1 expression is lost from the ventral region where radial glia (nestin$^+$) are lacking but is maintained at the dorsal boundary where radial glia still remain. Arrowheads indicate the end points of laminin-α1 expression. (P) Expression of laminin-α1 mRNA is lost in the ventral region of the double mutant. Scale bars: 100 μm in A,C,E,G,I-P; 100 μm in D,H; 10 μm in B,F.

E9.5 and 10.5 (Fig. 10C,E,F), whereas in the double-mutant neurons were already differentiated at E9.5 and 10.5 in the regions that should normally become optic vesicles (Fig. 10D,G), suggesting that accelerated neuronal differentiation may inhibit optic vesicle formation. The homeodomain gene *Rx*, which is essential for eye formation (Mathers et al., 1997), was expressed normally in *Hes1;Hes5* double-mutants, suggesting that the initial eye specification occurred in the double mutant (Fig. 10J). However, the downstream homeodomain genes *Pax2*, which specifies the optic stalk (Torres et al., 1996), and *Chx10*, which regulates retinal formation (Burmeister et al., 1996), were not expressed in the double mutant (Fig. 10K-N), suggesting that accelerated neuronal differentiation may hamper *Rx*-induced eye specification. Furthermore, the ganglionic eminences were not properly formed due to accelerated neuronal differentiation in *Hes1;Hes5* double mutants (Fig. 10B, compare with Fig. 10A, arrowhead). Thus, the normal timing of cell differentiation is essential for organization of proper structures such as the optic vesicles and the ganglionic eminences.

More severe defects in *Hes1-Hes3-Hes5* triple-mutant spinal cord

Although neuronal differentiation was severely accelerated in *Hes1;Hes5* double mutants, neuroepithelial cells were normally formed at E8.5 and radial glial cells still remained in the dorsal region (Figs 4 and 6), suggesting that a related bHLH gene may compensate for formation of neuroepithelial and dorsal radial glial cells. To determine whether or not *Hes* gene activities are required for these cells, we next examined another *Hes* gene, *Hes3*, which is also expressed in the developing nervous system (Allen and Lobe, 1999). At E8.0, like *Hes1*, *Hes3* was widely expressed in the nervous system (Fig. 11A,B,I) while *Hes5* was not (Fig. 11C). At E8.5-9.5, *Hes3* expression occurred widely (Fig. 11J,K) but was restricted to the medial to dorsal region (Fig. 11F,L), while *Hes5* and *Dll1* expression started in the ventral to medial region (Fig. 11G,H). After E9.5, *Hes3* expression is downregulated except for the isthmus (Hirata et al., 2001). In *Hes1;Hes5* double mutants, *Hes3* expression was not significantly affected (Fig. 11K-M).

Because *Hes3* may compensate for *Hes1* and *Hes5* deficiency in the formation of the neuroepithelium and the dorsal radial glia, we thus examined *Hes1;Hes3;Hes5* triple-mutant embryos. At E8.5, very few neurons (TuJ1$^+$) were generated in both the wild-type and *Hes1;Hes5* double-mutant embryos (Fig. 11N,O), whereas many neurons were prematurely differentiated in *Hes1;Hes3;Hes5* triple-mutant embryos (Fig. 11P). At this stage, although there were still many neuroepithelial cells in the triple mutant (nestin$^+$Ki67$^+$) (Fig. 11Q,R), they were not properly maintained and prematurely differentiated into neurons (Fig. 11P), suggesting that neuroepithelial cells are initially formed without *Hes* genes but become dependent on *Hes* gene activities by E8.5. At E9.5, most cells had become neurons in the ventral spinal cord of the triple mutant (Fig. 11S). Strikingly, at E10.0 virtually all radial glial cells (Ki67$^+$) were differentiated

into TuJ1$^+$ neurons in *Hes1;Hes3;Hes5* triple mutants (Fig. 11T-V), indicating that *Hes3* is responsible for dorsal radial glia and that the three *Hes* genes together are essential for maintenance of virtually all radial glial cells.

Discussion

Hes genes are essential for maintenance of neural stem cells

We demonstrated here that *Hes* genes are essential for organization of brain structure of appropriate size, shape and cell arrangement by maintaining neural stem cells. In the absence of *Hes* genes, cell differentiation is severely accelerated, leading to depletion of radial glial cells and resultant disorganization of the structural integrity of the nervous system. Interestingly, *Hes* genes are not required for the initial formation of neuroepithelial cells. However, in the absence of *Hes1*, *Hes3* and *Hes5*, neuroepithelial cells are not properly maintained but have prematurely differentiated into neurons by E8.5. Thus, neuroepithelial cells are initially

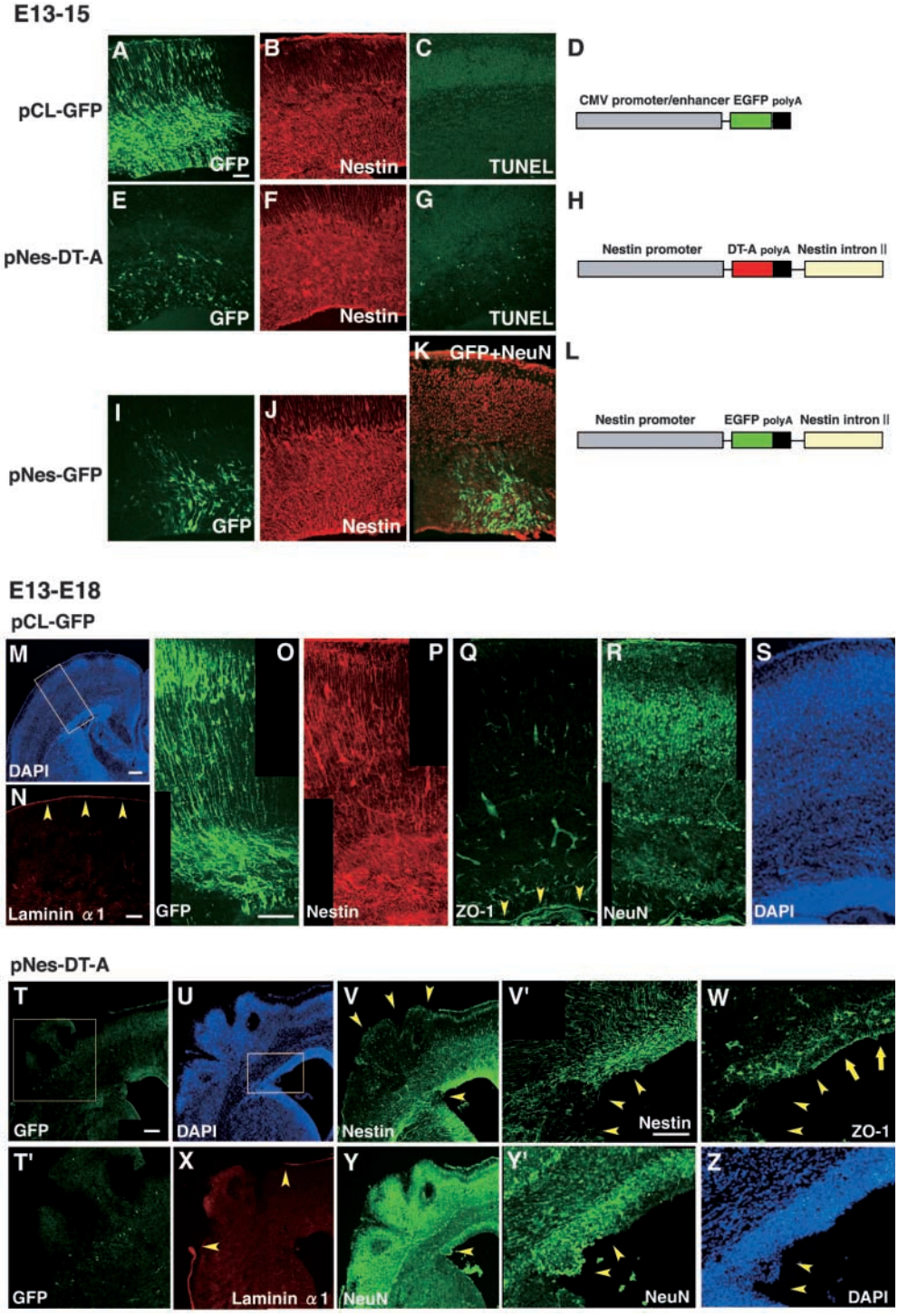

Fig. 9. Ablation of radial glia by diphtheria toxin (DT) disrupts the inner and outer barriers of the developing brain. (A-L) Each vector was introduced into the telencephalic cells by electroporation at E13, and the sections were examined at E15. When pCL-GFP was introduced (A-C), both cells in the ventricular zone (nestin$^+$) and the outer layers were found to express GFP. No dying cells (TUNEL$^+$) were detected (C). When pNes-DT-A was introduced (E-G), many cells underwent apoptosis in the ventricular zone (TUNEL$^+$, G). When pNes-GFP was introduced, only nestin$^+$ ventricular cells (I,J), but not NeuN$^+$ neurons (K), expressed GFP. The schematic structures of the vectors are shown in D,H,L. (M-Z) Each vector was introduced into the telencephalic cells by electroporation at E13, and the sections were examined at E18. When pCL-GFP was introduced (M-S), GFP was expressed in both radial glia and neurons (O) and did not affect radial glia (nestin$^+$, P), the apical junction (ZO-1$^+$, Q, arrowheads), the basal lamina (Laminin α1$^+$, N, arrowheads) or neurons (NeuN$^+$, R). Cell arrangement was not disturbed (DAPI, S). The indicated region in M is enlarged in O-S. When pNes-DT-A was introduced (T-Z), GFP$^+$ cells were almost undetectable (T,T′). Only a small number of GFP$^+$ neurons is detectable, which shows the electroporated region (T,T′). pNes-DT-A specifically killed nestin$^+$ radial glia, which disappeared from the electroporated region (V,V′, arrowheads). This region lost ZO-1 expression at the apical side (W, arrowheads, compare with the normal expression indicated by arrows). The electroporated region also lost laminin α1 at the basal side (X, between the two arrowheads). In this region, the cortical lamination is destroyed with rosette-like structures, and some neurons protrude into the outer region and the lumen (Y,Y′,Z, arrowheads). The indicated region in (T) and (U) is enlarged in (T′) and (V′,W,Y′,Z), respectively. Scale bars: 100 μm in A-C,E-G,I-K,N-S,T',V′,W,Y′,Z; 200 μm M,T-V,X,Y.

independent of, but become dependent on, *Hes* gene activities for their maintenance before changing to radial glia. In the wild type, radial glial cells undergo an asymmetric cell division, forming one radial glial cell and one neuron from each cell division. In the absence of *Hes* genes, however, radial glial cells seem to be unable to undergo asymmetric cell division, forming neurons only. Thus, *Hes* genes are essential for maintenance of both neuroepithelial and radial glial cells. These observations also indicate that neural stem cells change their characters over time, in the following order: *Hes*-independent neuroepithelial cells, transitory *Hes*-dependent neuroepithelial cells, and *Hes*-dependent radial glial cells (Fig. 12A). Based on the expression patterns (Fig. 11), transitory *Hes*-dependent neuroepithelial cells seem to depend on *Hes1* and *Hes3*, while *Hes*-dependent radial glial cells mostly depend on *Hes1* and *Hes5* (Fig. 12A), although dorsal radial glial cells depend on *Hes3* to some extent.

Hes genes organize the brain structures by maintaining radial glial cells

Radial glial cells form intercellular junctions at the apical side and basal lamina at the basal side (Fig. 12B, part a). We showed that premature loss of radial glial cells disrupts both the apical intercellular junction and the basal lamina and allows neurons scattered into the lumen and to the outer regions (Fig. 12B, part b). Because radial glial cells guide neuronal migration, loss of radial glia should lead to aberrant neuronal localization and disruption of the mantle layers. However, if the apical junctions and the basal lamina are maintained, they should block cells and keep them inside the wall of the neural tube. Thus, radial glial cells establish the framework of the neural tube by forming the inner and outer barriers, which are essential for maintenance of the neural tube morphology. These results indicate that radial glial cells play multiple roles in constructing the nervous system: serving as neural stem cells, guiding neuronal migration and forming the inner and outer barriers.

Radial glial cells form intercellular junctions at the apical side

Previous morphological analyses show conflicting results about the presence of the tight junction (Aaku-Saraste et al., 1996; Bancroft and Bellairs, 1975; Decker and Friend, 1974; Duckett, 1968; Hinds and Ruffett, 1971; Møllgård et al., 1987; Revel and Brown, 1975). It was previously shown that, during neurulation, expression of the tight junction molecule occludin is lost (Aaku-Saraste et al., 1996). In the present study, however, we found that the tight junction did exist at the apical side of the neural tube on TEM analysis and that the tight junction molecules claudins were expressed by radial glial cells on immunohistochemical analysis. Thus, it is most likely that, even after neurulation, radial glial cells are anchored at the apical side by the tight junction as well as by the adherens junction. We speculate that a single strand junction identified by the freeze-fracture method (Møllgård et al., 1987) may correspond to a claudin-based tight junction. Further analysis is required to determine the features of the tight junction of the embryonal nervous system.

It was previously shown that blockade of N-cadherin activity by specific antibody or gene inactivation destroys the laminar structure of the nervous system, indicating an essential role of N-cadherin in maintenance of the nervous system morphology (Bronner-Fraser et al., 1992; Gänzler-Ordenthal and Redies, 1998; Lele et al., 2002; Luo et al., 2001; Masai et al., 2003). However, because N-cadherin is diffusely expressed by almost all neural cells including neurons, blockade of N-cadherin activity may disrupt interactions between all these cells, making it difficult to interpret the contribution of radial glial cells to the structural integrity. In the present study, we showed that, although neurons still expressed N-cadherin, loss of radial glial cells scattered many neurons out of the neural tube, indicating that diffuse N-

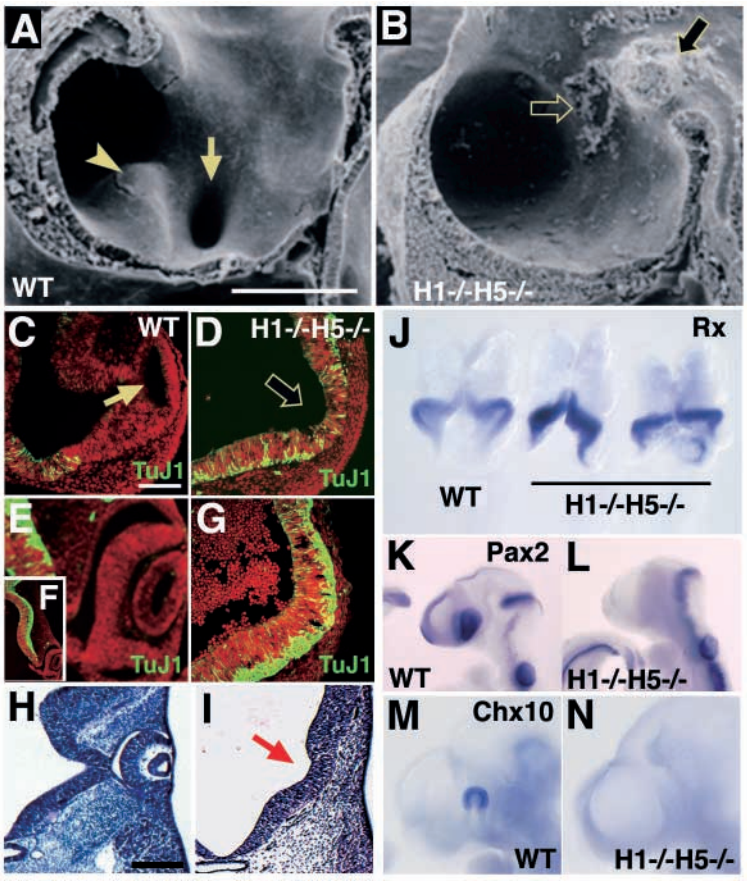

Fig. 10. Lack of the optic vesicles and the ganglionic eminences in *Hes1;Hes5* double-mutant brain. (A,B) SEM analysis shows the optic vesicle (arrow) and the ganglionic eminence (arrowhead) in the wild type (A) while such structures are not formed in the *Hes1;Hes5* double-mutant brain (B). In some regions, cell arrangement is disrupted (B, arrows). (C-G) Immunohistochemistry for TuJ1. Neurons ($TuJ1^+$, green) are not generated in the wild type optic vesicle at E9.5 (C) and E10.5 (E,F). By contrast, in *Hes1;Hes5* double-mutants, neurons are already differentiated at E9.5 (D) and E10.5 (G) in the region that should normally become optic vesicles. The nuclei are counterstained with PI (red). (H,I) HE staining of the wild type (H) and *Hes1;Hes5* double mutant (I). In the double mutant, the eye is not formed (I, arrow). (J) *Rx* is expressed similarly in both the wild type and *Hes1;Hes5* double-mutant. (K-N) *Pax2* and *Chx10* are expressed in the wild-type eye (K,M) but not in the double-mutant (L,N). Scale bars: 500 μm in A,B; 100 μm in C-E,G; 200 μm in H,I.

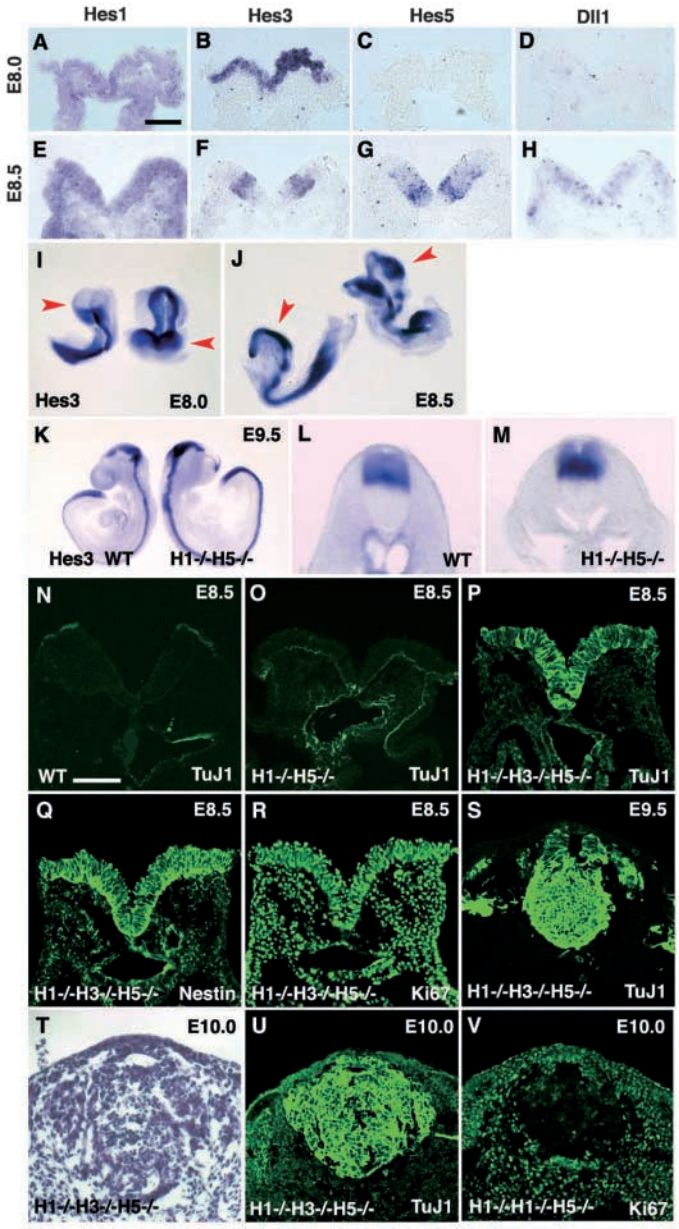

Fig. 11. Premature loss of neuroepithelial and radial glial cells in *Hes1;Hes3;Hes5* triple mutants. (A-D) At E8.0, like *Hes1* (A), *Hes3* is expressed in the nervous system (B) whereas *Hes5* and *Dll1* are not (C,D). (E-H) At E8.5, while *Hes1* is still diffusely expressed (E), *Hes3* expression domain is restricted to the medial to dorsal region (F). *Hes5* and *Dll1* expression is observed at this stage (G,H). (I,J) *Hes3* is widely expressed in the developing nervous system at E8.0 (I) and E8.5 (J). The head region is indicated by arrowheads. (K-M) *Hes3* expression is not significantly affected in the *Hes1;Hes5* double mutant, compared with the wild type. (N-R) At E8.5, very few neurons (TuJ1^{+}) are generated in both the wild type and *Hes1;Hes5* double mutant (N,O) whereas in *Hes1;Hes3;Hes5* triple-mutant, many neurons are prematurely differentiated (P). There are still many neuroepithelial cells (nestin^{+}Ki67^{+}) in the *Hes1;Hes5* double mutant (Q,R). (S) At E9.5, more neurons are prematurely differentiated in the ventral region of *Hes1;Hes3;Hes5* triple-mutant spinal cord. (T-V) At E10.0, the structure of the spinal cord is severely disorganized in *Hes1;Hes3;Hes5* triple mutants (T). Strikingly, virtually all cells become neurons (U), and radial glia are missing (V). Scale bars: 100 μm in A-H,N-V.

cadherin expression is not sufficient to keep neurons inside the wall of the neural tube.

Radial glial cells contribute to the basal lamina formation

The basal lamina is composed of networks of glycoproteins such as laminin and collagen IV (Timpl, 1996; Yurchenco and O'Rear, 1994). It was previously shown that laminin is expressed by radial glial cells (Liesi, 1985; Thomas and Dziadek, 1993). We found that, when radial glial cells disappear, both laminin-α1 mRNA in the ventricular zone and laminin-α1 protein at the basal side are lost or severely downregulated. These results suggest that radial glial cells produce, transport, and secrete laminin-α1 to the basal side. The phenotype of radial glial cell loss is very similar to that of laminin-γ1-mutant mice, which display disruption of the basal lamina and neuronal protrusion through the meninges (Halfter

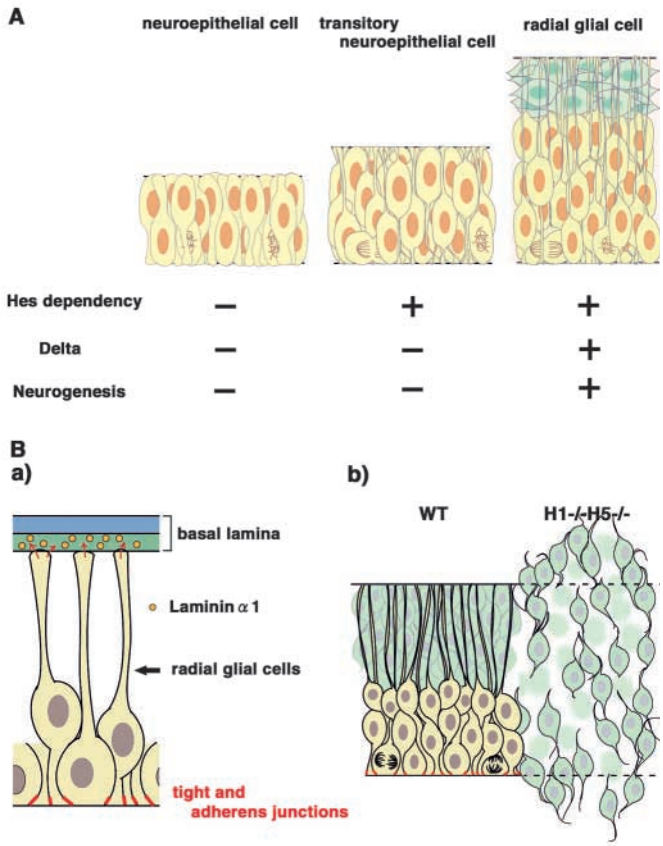

Fig. 12. Characters and functions of neural stem cells. (A) Embryonic neural stem cells change their characters in the following order: *Hes*-independent neuroepithelial cells, transitory *Hes*-dependent neuroepithelial cells, and *Hes*-dependent radial glial cells. Based on the expression patterns, transitory *Hes*-dependent neuroepithelial cells seem to depend on *Hes1* and *Hes3*, while *Hes*-dependent radial glial cells mostly depend on *Hes1* and *Hes5*. (B) Roles of radial glia in the inner and outer barrier formation. (a) Radial glia form the tight and adherens junctions at the apical side and contribute to the basal lamina formation at the basal side. (b) Radial glia establish the framework of the neural tube by forming the inner and outer barriers. In the absence of radial glia (*Hes1*$^{-/-}$;*Hes5*$^{-/-}$), neurons escape from the wall of the neural tube, thereby destroying the structural integrity.

et al., 2002). Radial glial cells thus contribute to formation of the outer barrier by expressing laminin.

Previous studies showed that the collagen IV network is produced by surrounding mesenchymal cells but not by radial glial cells (Thomas and Dziadek, 1993). In addition, in-situ hybridization analysis showed that laminin-α1 mRNA is weakly expressed by surrounding mesenchymal cells next to the spinal cord. Thus, the basal lamina is generated cooperatively at the interface by radial glia and mesenchymal cells.

Accelerated differentiation generates neurons at the expense of the later-born cell types in the absence of *Hes* genes

Neural stem cells are known to change their competency over time (Desai and McConnell, 2000). They initially give rise to neurons and later to other cell types such as ependymal cells and astrocytes. Ependymal cells are the internal lining of the neural tube and carry the adherens junction (Lagunowich et al., 1992; Møllgård et al., 1987; Redies et al., 1993), while astrocytes produce laminin (Liesi et al., 1983). Thus, in the wild type, at later stages when radial glial cells disappear, they are replaced by ependymal cells and astrocytes.

In *Hes*-null mice, differentiation of radial glial cells is accelerated. There could be two types of acceleration: (1) all cell types are generated rapidly; or (2) only early-born cell types are generated at the expense of the later-born cell types. In *Hes*-null mice, radial glial cells prematurely differentiate into neurons only without giving rise to later-born cell types. It is likely that it takes a certain period of time for neural stem cells to change their competency to generate the later-born cell types. It was previously shown that the promoter region of the astrocyte-specific gene for glial fibrillary acidic protein (GFAP) is highly methylated and silenced in neural stem cells at early stages of development (Takizawa et al., 2001). Neural stem cells at early stages are therefore refractory to inductive signals for astrocyte differentiation. However, as development proceeds, the GFAP promoter region is gradually demethylated, and neural stem cells gain the competency to become astrocytes. Thus, maintenance of radial glial cells for a certain period of time during development has two functions: increasing the cell number; and covering a full range of competency. Accelerated differentiation therefore leads to defects in both aspects, reduction of the cell number and lack of later-born cell types.

We thank Drs Sue McConnell and Toshiyuki Ohtsuka for discussion and critical reading of an early version of the manuscript, Drs Shoichiro Tsukita and Mikio Furuse for providing antibodies, discussion and technical advice and Dr Makoto Ishibashi for technical help. This work was supported by research grants from the Ministry of Education, Culture, Sports, Science and Technology of Japan and the Japan Society for the Promotion of Science. J.H. was supported by Research Fellowships of the Japan Society for the Promotion of Science for Young Scientists.

References

Aaku-Saraste, E., Hellwig, A. and Huttner, W. B. (1996). Loss of occludin and functional tight junctions, but not ZO-1, during neural tube closure – remodeling of the neuroepithelium prior to neurogenesis. *Dev. Biol.* **180**, 664-679.

Allen, T. and Lobe, C. G. (1999). A comparison of *Notch*, *Hes* and *Grg* expression during murine embryonic and post-natal development. *Cell. Mol. Biol.* **45**, 687-708.

Artavanis-Tsakonas, S., Rand, M. D. and Lake, R. J. (1999). Notch signaling: cell fate control and signal integration in development. *Science* **284**, 770-776.

Bancroft, M. and Bellairs, R. (1975). Differentiation of the neural plate and neural tube in the young chick embryo. *Anat. Embryol.* **147**, 309-335.

Bronner-Fraser, M., Wolf, J. J. and Murray, B. A. (1992). Effects of antibodies against N-cadherin and N-CAM on the cranial neural crest and neural tube. *Dev. Biol.* **153**, 291-301.

Burmeister, M., Novak, J., Liang, M.-Y., Basu, S., Ploder, L., Hawes, N. L., Vidgen, D., Hoover, F., Goldman, D., Kalnins, V. I. et al. (1996). Ocular retardation mouse caused by *Chx10* homeobox null allele: impaired retinal progenitor proliferation and bipolar cell differentiation. *Nat. Genet.* **12**, 376-384.

Castella, P., Sawai, S., Nakao, K., Wagner, J. A. and Caudy, M. (2000). HES-1 repression of differentiation and proliferationin PC12 cells: role for the helix 3-helix 4 domain in transcription repression. *Mol. Cell. Biol.* **20**, 6170-6183.

Cau, E., Gradwohl, G., Casarosa, S., Kageyama, R. and Guillemot, F. (2000). *Hes* genes regulate sequential stages of neurogenesis in the olfactory epithelium. *Development* **127**, 2323-2332.

Chenn, A. and Walsh, C. A. (2002). Regulation of cerebral cortical size by control of cell cycle exit in neural precursors. *Science* **297**, 365-369.

Conlon, R. A., Reaume, A. G. and Rossant, J. (1995). *Notch1* is required for the coordinate segmentation of somites. *Development* **121**, 1533-1545.

Decker, R. S. and Friend, D. S. (1974). Assembly of gap junctions during amphibian neurulation. *J. Cell Biol.* **62**, 32-47.

Desai, A. R. and McConnell, S. K. (2000). Progressive restriction in fate potential by neural progenitors during cerebral cortical development. *Development* **127**, 2863-2872.

Duckett, S. (1968). The germinal layer of the growing human brain during early fetal life. *Anat. Rec.* **161**, 231-246.

Fantl, V., Stamp, G., Andrews, A., Rosewell, I. and Dickson, C. (1995). Mice lacking cyclin D1 are small and show defects in eye and mammary gland development. *Genes Dev.* **9**, 2364-2372.

Fero, M. L., Rivkin, M., Tasch, M., Porter, P., Carow, C. E., Firpo, E., Polyak, K., Tsai, L.-H., Broudy, V., Perlmutter, R. M. et al. (1996). A syndrome of multiorgan hyperplasia with features of gigantism, tumorigenesis, and female sterility in $p27^{Kip1}$-deficient mice. *Cell* **85**, 733-744.

Fujita, S. (1964). Analysis of neuron differentiation in the central nervous system by tritiated thymidine autoradiography. *J. Comp. Neurol.* **122**, 311-327.

Gaiano, N. and Fishell, G. (2002). The role of Notch in promoting glial and neural stem cell fates. *Annu. Rev. Neurosci.* **25**, 471-490.

Gänzler-Ordenthal, S. I. I. and Redies, C. (1998). Blocking N-cadherin function disrupts the epithelial structure of differentiating neural tissue in the embryonic chicken brain. *J. Neurosci.* **18**, 5415-5425.

Geng, Y., Yu, Q., Sicinska, E., Das, M., Schneider, J. E., Bhattacharya, S., Rideout, W. M., Bronson, R. T., Gardner, H. and Sicinski, P. (2003). Cyclin E ablation in the mouse. *Cell* **114**, 431-443.

Halfter, W., Dong, S., Yip, Y.-P., Willem, M. and Mayer, U. (2002). A critical function of the pial basement membrane in cortical histogenesis. *J. Neurosci.* **22**, 6029-6040.

Hamada, Y., Kadowaki, Y., Okabe, M., Ikawa, M., Coleman, J. R. and Tsujimoto, Y. (1999). Mutation in ankyrin repeats of the mouse *Notch2* gene induces early embryonic lethality. *Development* **126**, 3415-3424.

Hatakeyama, J., Tomita, K., Inoue, T. and Kageyama, R. (2001). Roles of homeobox and bHLH genes in specification of a retinal cell type. *Development* **128**, 1313-1322.

Hatta, K. and Takeichi, M. (1986). Expression of N-cadherin adhesion molecules associated with early morphogenetic events in chick development. *Nature* **320**, 447-449.

Hayashi, K., Yonemura, S., Matsui, T., Tsukita, S. and Tsukita, S. (1999). Immunofluorescence detection of ezrin/radixin/moesin (ERM) proteins with their carboxyl-terminal threonine phosphorylated in cultured cells and tissues. *J. Cell Sci.* **112**, 1149-1158.

Hinds, J. W. and Ruffett, T. L. (1971). Cell proliferation in the neural tube: an electron microscopic and Golgi analysis in the mouse cerebral vesicle. *Z. Zellforsch.* **115**, 226-264.

Hirata, H., Ohtsuka, T., Bessho, Y. and Kageyama, R. (2000). Generation

of structurally and functionally distinct factors from the basic helix-loop-helix gene *Hes3* by alternative first exons. *J. Biol. Chem.* **275**, 19083-19089.

Hirata, H., Tomita, K., Bessho, Y. and Kageyama, R. (2001). *Hes1* and *Hes3* regulate maintenance of the isthmic organizer and development of the mid/hindbrain. *EMBO J.* **20**, 4454-4466.

Hitoshi, S., Alexson, T., Tropepe, V., Donoviel, D., Elia, A. J., Nye, J. S., Conlon, R. A., Mak, T. W., Bernstein, A. and van der Kooy, D. (2002). Notch pathway molecules are essential for the maintenance, but not the generation, of mammalian neural stem cells. *Genes Dev.* **16**, 846-858.

Honjo, T. (1996). The shortest path from the surface to the nucleus: RBP-J κ/Su(H) transcription factor. *Genes Cells* **1**, 1-9.

Huard, J. M. T., Forster, C. C., Carter, M. L., Sicinski, P. and Ross, E. M. (1999). Cerebellar histogenesis is disturbed in mice lacking cyclin D2. *Development* **126**, 1927-1935.

Kabos, P., Kabosoba, A. and Neuman, T. (2002). Blocking HES1 expression initiates GABAergic differentiation and induces the expression of $p21^{CIP1/WAF1}$ in human neural stem cells. *J. Biol. Chem.* **277**, 8763-8766.

Kageyama, R. and Nakanishi, S. (1997). Helix-loop-helix factors in growth and differentiation of the vertebrate nervous system. *Curr. Opin. Genet. Dev.* **7**, 659-665.

Kiuchi-Saishin, Y., Gotoh, S., Furuse, M., Takasuga, A., Tano, Y. and Tsukita, S. (2002). Differential expression patterns of Claudins, tight junction membrane proteins, in mouse nephron segments. *J. Am. Soc. Nephrol.* **13**, 875-886.

Lagunowich, L. A., Schneider, J. C., Chasen, S. and Grunwald, G. B. (1992). Immunohistochemical and biochemical analysis of N-cadherin expression during CNS development. *J. Neurosci. Res.* **32**, 202-208.

Lele, Z., Folchert, A., Concha, M., Rauch, G.-J., Geisler, R., Rosa, F., Wilson, S. W., Hammerschmidt, M. and Bally-Cuif, L. (2002). *parachute/n-cadherin* is reguired for morphogenesis and maintained integrity of the zebrafish neural tube. *Development* **129**, 3281-3294.

Liesi, P. (1985). Do neurons in the vertebrate CNS migrate on laminin? *EMBO J.* **4**, 1163-1170.

Luo, Y., Ferreira-Cornwell, M. C., Baldwin, H. S., Kostetskii, I., Lenox, J. M., Lieberman, M. and Radice, G. L. (2001). Rescuing the N-cadherin knockout by cardiac-specific expression of N- or E-cadherin. *Development* **128**, 459-469.

Masai, I., Lele, Z., Yamaguchi, M., Komori, A., Nakata, A., Nishiwaki, Y., Wada, H., Tanaka, H., Nojima, Y., Hammerschmidt, M. et al. (2003). N-cadherin mediates retinal lamination, maintenance of forebrain compartments and patterning of retinal neurites. *Development* **130**, 2479-2494.

Mathers, P. H., Grinberg, A., Mahon, K. A. and Jamrich, M. (1997). The *Rx* homeobox gene is essential for vertebrate eye development. *Nature* **387**, 603-607.

McConnell, S. K. (1995). Constructing the cerebral cortex: neurogenesis and fate determination. *Neuron* **15**, 761-768.

Møllgård, K., Balslev, Y., Lauritzen, B. and Saunders, N. R. (1987). Cell junctions and membrane specializations in the ventricular zone (germinal matrix) of the developing sheep brain: a CSF-brain barrier. *J. Neurocytol.* **16**, 433-444.

Nakamura, Y., Sakakibara, S., Miyata, T., Ogawa, M., Shimazaki, T., Weiss, S., Kageyama, R. and Okano, H. (2000). The bHLH gene *Hes1* as a repressor of the neuronal commitment of CNS stem cells. *J. Neurosci.* **20**, 283-293.

Nakayama, K., Ishida, N., Shirane, M., Inomata, A., Inoue, T., Shishido, N., Horii, I., Loh, D. Y. and Nakayama, K. (1996). Mice lacking $p27^{Kip1}$ display increased body size, multiple organ hyperplasia, retinal dysplasia, and pituitary tumors. *Cell* **85**, 707-720.

Ohnuma, S. and Harris, W. A. (2003). Neurogenesis and the cell cycle. *Neuron* **40**, 199-208.

Ohtsuka, T., Ishibashi, M., Gradwohl, G., Nakanishi, S., Guillemot, F. and Kageyama, R. (1999). *Hes1* and *Hes5* as Notch effectors in mammalian neuronal differentiation. *EMBO J.* **18**, 2196-2207.

Ohtsuka, T., Sakamoto, M., Guillemot, F. and Kageyama, R. (2001). Roles of the basic helix-loop-helix genes *Hes1* and *Hes5* in expansion of neural stem cells of the developing brain. *J. Biol. Chem.* **276**, 30467-30474.

Qian, X., Shen, Q., Goderie, S. K., He, W., Capela, A., Davis, A. A. and Temple, S. (2000). Timing of CNS cell generation: a programmed sequence of neuron and glial cell production from isolated murine cortical stem cells. *Neuron* **28**, 69-80.

Redies, C., Engelhart, K. and Takeichi, M. (1993). Differential expression of N- and R-cadherin in functional neuronal systems and other structures of the developing chicken brain. *J. Comp. Neurol.* **333**, 398-416.

Revel, J.-P. and Brown, S. S. (1975). Cell junctions in development, with particular reference to the neural tube. *Cold Spring Harbor Symp. Quant. Biol.* **40**, 443-455.

Selkoe, D. and Kopan, R. (2003). Notch and presenilin: regulated intramembrane proteolysis links development and degeneration. *Annu. Rev. Neurosci.* **26**, 565-597.

Sherr, C. J. and Roberts, J. M. (1999). Inhibitors of mammalian G_1 cyclin-dependent kinases. *Genes Dev.* **9**, 1149-1163.

Sicinski, P., Donaher, J. L., Parker, S. B., Li, T., Fazeli, A., Gardner, H., Haslam, S. Z., Bronson, R. T., Elledge, S. J. and Weinberg, R. A. (1995). Cyclin D1 provides a link between development and oncogenesis in the retina and breast. *Cell* **82**, 621-630.

Swiatek, P. J., Lindsell, C. E., del Amo, F. F., Weinmaster, G. and Gridley, T. (1994). *Notch1* is essential for postimplantation development in mice. *Genes Dev.* **8**, 707-719.

Takizawa, T., Nakashima, K., Namihira, M., Ochiai, W., Uemura, A., Yanagisawa, M., Fujita, N., Nakao, M. and Taga, T. (2001). DNA methylation is a critical cell-intrinsic determinant of astrocyte differentiation in the fetal brain. *Dev. Cell* **1**, 749-758.

Temple, S. (2001). The development of neural stem cells. *Nature* **414**, 112-117.

Thomas, T. and Dziadek, M. (1993). Genes coding for basement membrane glycoproteins laminin, nidogen, and collagen IV are differentially expressed in the nervous system and by epithelial, endothelial, and mesenchymal cells of the mouse embryo. *Exp. Cell Res.* **208**, 54-67.

Timpl, R. (1996). Macromolecular organization of basement membranes. *Curr. Opin. Cell Biol.* **8**, 618-624.

Tomita, K., Ishibashi, M., Nakahara, K., Ang, S.-L., Nakanishi, S., Guillemot, F. and Kageyama, R. (1996). Mammalian *hairy* and *Enhancer of split* homolog 1 regulates differentiation of retinal neurons and is essential for eye morphogenesis. *Neuron* **16**, 723-734.

Torres, M., Gómez-Pardo, E. and Gruss, P. (1996). Pax2 contributes to inner ear patterning and optic nerve trajectory. *Development* **122**, 3381-3391.

Tsukita, S., Furuse, M. and Itoh, M. (2001). Multifunctional strands in tight junctions. *Nat. Rev. Mol. Cell. Biol.* **2**, 285-293.

Yamaizumi, M., Mekada, E., Uchida, T. and Okada, Y. (1978). One molecule of diphtheria toxin fragment A introduced into a cell can kill the cell. *Cell* **15**, 245-250.

Yurchenco, P. D. and O'Rear, J. J. (1994). Basal lamina assembly. *Curr. Opin. Cell Biol.* **6**, 674-681.

Zimmerman, L., Lendahl, U., Cunningham, M., Mckay, R., Parr, B., Gavin, B., Mann, J., Vassileva, G. and McMahon, A. (1994). Independent regulatory elements in the nestin gene direct transgene expression to neural stem cells or muscle precursors. *Neuron* **12**, 11-24.